Available online at www.sciencedirect.com

ScienceDirect

Ciência & Tecnologia dos Materiais 29 (2017) e56–e61

Ciência & Tecnologia dos MATERIAIS

http://ees.elsevier.com/ctmat

Special Issue "Materiais 2015"

Residual stress field and distortions resulting from welding processes: numerical modelling using Sysweld

Tiago R. Lima[a], Sérgio M.O. Tavares[b, *], Paulo M.S.T. de Castro[a]

[a]*FEUP, Universidade do Porto, Rua Dr. Roberto Frias s/n, 4200-465 Porto, Portugal*
[b]*INEGI, Universidade do Porto, Campus FEUP, Rua Dr. Roberto Frias 400, 4200-465 Porto, Portugal*

Abstract

This paper concerns the study of residual stresses and distortions in fusion butt joint welding, using the computational modelling software ESI Sysweld. Thermal gradients across the part will introduce geometrical variations that cause residual stress and distortions; their study and prediction are critical to ensure a sound welding.
To foresee the welding behaviour is a complex task because there are many physical-chemical phenomena involved in the welding processes. Using Sysweld - a finite element method based software - it is possible to integrate all the physical-chemical phenomena and elaborate computational models for most welding cases.
A real case consisting of three sets of aluminium plates welded by laser will be studied in this paper. A finite element model is realized for each case and the results are analysed using Sysweld capabilities.

© 2017 Portuguese Society of Materials (SPM). Published by Elsevier España, S.L.U. All rights reserved.

Keywords: Finite element method (FEM); residual stress; distortion; Sysweld; welding simulation.

1. Introduction

Welding is an effective joining process for a wide range of applications, allowing to join parts permanently in a fast and economic way and, at the same time, with adequate mechanical properties.
However, the uneven heating resulting from welding processes combined with mechanical restrictions from clamping systems leads to significant stresses in the weldment area and distortions in the work piece [1]. These distortions are interrelated to the residual stresses and occur in the presence of some kind of restraint condition. It is not possible to separate both phenomena; there is an interrelationship between them, shown in Fig. 1. Many efforts are made to predict and correct these phenomena, like varying the welding sequence and clamping conditions [3].

* Corresponding author.
E-mail address: sergio.tavares@fe.up.pt (S.M.O. Tavares)

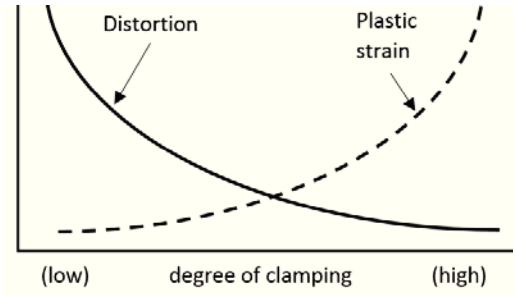

Fig. 1. Relationship between distortions and plastic strains as a function of degree of clamping. Adapted from [2].

1.1. Welding computational simulation

Computational modelling, based on finite element method theory, enables the virtual examination of the distortion and can verify the influence of the welding sequence, direction and boundary conditions effects, supporting a faster process development and improved welding parameters [3].

© 2017 Portuguese Society of Materials (SPM). Published by Elsevier España, S.L.U. All rights reserved.
http://dx.doi.org/10.1016/j.ctmat.2016.07.015

Sysweld simulates the physical phenomena occurring in the welding process. The thermal analysis is based on transient thermal conduction model. The heat source is the main difference between different welding processes. Heat sources, like double ellipsoid, are typical for welding processes such electric arc, MIG and TIG. High power welding processes use beam sources, characterized by a Gaussian temperature distribution [2].
This paper presents a case study of simulation of residual stresses in a simple butt laser beam weldment, using a numerical tool dedicated to welding processes modelling.

1.2. Residual stress distribution

In a 2D planar case, the static equilibrium condition implies that the tensile residual stress area needs to be equal to the compressive residual stress area. The usual schematic diagram for butt joint residual stress distribution is presented *e.g.* by K. Masubuchi [4] and it is schematically shown in Fig. 2.

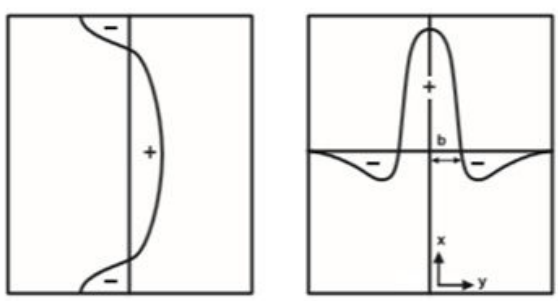

Fig. 2. Transversal residual stress (a) and longitudinal residual stress (b) [4,5].

Using simulations tools, as Sysweld, it is possible to predict residual stress field for different welding processes and for complex geometries, allowing a better decision about the best suitable process for a given purpose, as presented in the study of Zaeh and Roeren [6], comparing a Nd:YAG-laser with a high power diode laser (HPDL) for an aluminium profile welding.

2. Case Study

The numerical study is based on an experimental work of laser beam welding in thin aluminium alloy sheets, using a fiber laser Nd:YAG of 400W [7].
The sample dimensions and Al alloys used are listed in Table 1. Fig. 3 presents the samples after welding. These samples were measured and characterized to provide inputs for the computational analysis using Sysweld.

Table 1. Welded samples characteristics.

Test name	Welding type	Material	Dimensions (width x length x thickness) (mm)
Set I	Laser	AA5083	2x(20x123x1)
Set VII	Laser	AA6082	2x(20x123x1)
Set VIII	Laser	AA5083 and AA6082	(20x123x1)+(20x123x0.8)

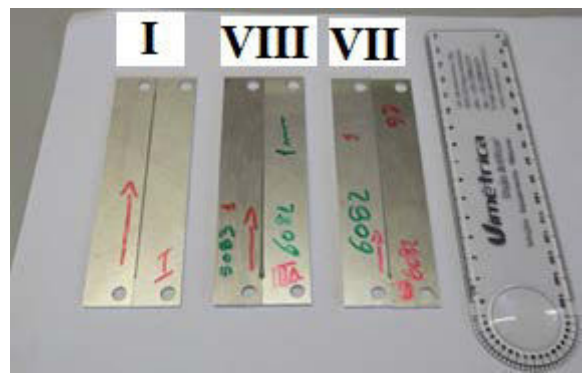

Fig. 3. Aluminium alloy welded samples.

2.1. Boundary conditions

Fig. 4 shows the welding set-up, in particular the two rectangular cross section tubes used for clamping. These tubes are of sufficient stiffness to be considered rigid.
In the finite element model, the nodes were restrained in the vertical direction due to the grip system adopted, as shown in Fig. 4. Therefore, it is assumed that the vertical movement of the plates during the process, in the grip region, can be neglected.
The contact conditions and external forces were also neglected since they originate a numerical complex problem during the transient state and their effect on the residual stress is minor. A two phase clamping condition was adopted in the simulation. The first phase considers the time during the welding process (Fig. 5) and the second phase refers to the cooling stage (Fig. 6). For each phase a time period of 30s was adopted.
The already mentioned tubes were fixed in the working table; so, the top surface clamping condition consists in two columns of nodes where all directions were fixed (Fig. 4).

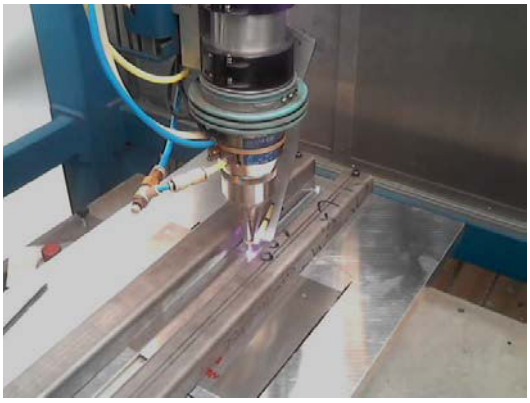

Fig. 4. Welding process at initial moment.

In the bottom surface, all nodes are only fixed in the vertical direction. This approach is a simplification because in the real case scenario the external edges of the part can rotate. In the cooling clamping phase, the part was unconstrained.

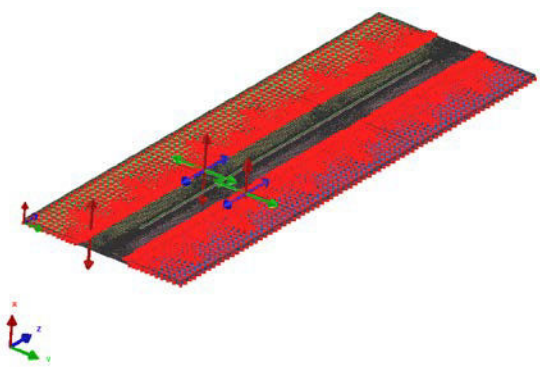

Fig. 5. Clamping condition – stage 1.

The part is air cooled at room temperature (20ºC). Contact conditions and external forces are not considered.

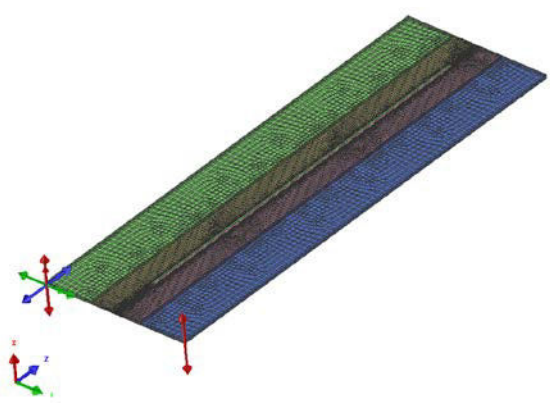

Fig. 6. Clamping condition - stage 2.

3. Finite Element Models and Weld Simulations

The Finite Element (FE) mesh was created in Visual Mesh. Initial work was performed concerning element type and size for this type of simulation, and it was concluded that the tetrahedral quadratic elements give good results compared with hexahedral elements, if the mesh is refined near the welding line. This type of mesh gives greater geometrical flexibility and facilitates to perform transitions between coarse to refined meshes.

Due to the small plate thickness, 2D shell elements could be used. However, 3D solid tetrahedral elements were used to obtain precise results and information along the thickness. An equal mesh was adopted in plate sets I and VII due to the similar geometry and to unify the results. For the plate set VIII, the model suffered some adjustments to join two different plate thicknesses. The meshes were divided in three equal portions to facilitate the mesh generation and the post-processing treatment.

Welding speed and torch angle values were considered constant in order to simplify the model data. Although a section cut, transverse to the welding bead and respective microscopic analysis was not performed, it is possible to see in the part surfaces the irregularity of the welding bead: full penetration accompanied with large width at the start and thin weld width with uncertain penetration along most of the welding.

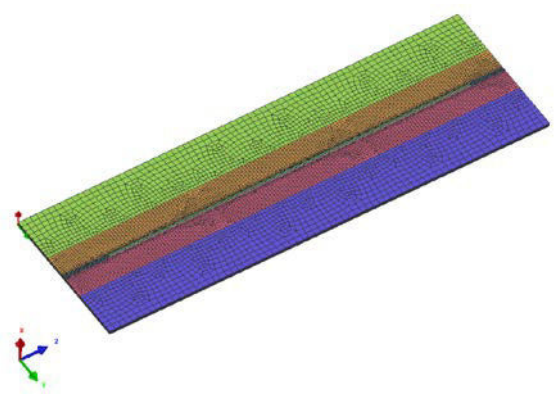

Fig. 7. Finite element mesh for real case I and VII.

To simplify the study, the weld nugget geometry was considered constant all over the weld line with a half thickness penetration.

Sysweld material database does not include the exact AA6082 aluminium alloy; so, the software standard 6000 alloy series was adopted.

Table 2. Experimental welding values.

	Set I	Set VII	Set VIII
Material	AA5083	AA6082	AA5083 and AA6082
Thickness (mm)	1	1	1 (left) and 0.8 (right)
Welding speed (mm/s)	30	30	20
Torch angle (º)	90	90	90

The Sysweld model needs to be calibrated in order to optimize the welding behaviour and the welding nugget geometry. The iterative process gave the results presented in Table 3. This table shows the properties of the heat source (double ellipsoid), obtained after model calibration.

Table 3. Heat source parameters used in Sysweld for the simulation.

	Set I	Set VII	Set VIII
Welding speed (mm/s)	30	30	20
Top beam diameter (mm)	1	1	1
Root beam diameter (mm)	0.2	0.2	0.2
Heat source penetration (mm)	0.1	0.1	0.1
Energy per unit length (J/mm)	18	18	18
Efficiency (%)	44	44	44

The energy input per unit length and efficiency were defined during Sysweld model calibration considering laser power adjustment and welding speed [2]; the efficiency value used is of the same order as the value used by other authors, 0.37 [8].
Thermal conductivity is considered in the simulations, considering steel in the backing table and in the restrained areas, and air in the remaining areas. Sysweld contains a significant material database and, for the present case, the thermal conductivity considered is function of the temperature.

4. Results

Sysweld is a FEM based software that can give a transient solution for multiple related welding phenomena. In this paper, just residual stresses will be shown; however, thermo-metallurgical analysis should be mentioned as essential to understand the welding effects in the part.
Thermal analysis is very important to ensure the correct implementation of the computational model. Thus, the desired weld bead geometry may correspond to the melting area obtained after the model calibration.

Longitudinal residual stress results were obtained in a cross section at 1/3 of the plate length.

4.1. Residual stress distribution

4.1.1. Plate set 1

The distribution of the longitudinal residual stress is similar in the top and in the bottom surfaces (Fig. 8). Both peak values are approximately 200 MPa. The areas away from the welding line present compressive values of stress, resulting from the material expansion in the weld line, followed by fast cooling. The maximum tension occurs in the thermal affected zone and the welding line was subjected to stress relief.

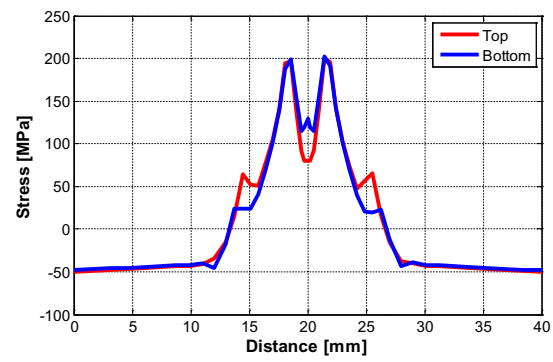

Fig. 8. Longitudinal residual stress. Plate set I. (distance is measured along the width, from the left side; width of each welded part is 20 mm, see Table 1).

The transverse residual stress at top surface is higher in a small amount than the values presented in the bottom surface (Fig. 9). The compressive values presented in the majority of the weld length will origin a convex shape in the part, similar to the results obtained by Zain-ul-Abdein *et al.* [9], for laser beam welding of AA6056 sheets.

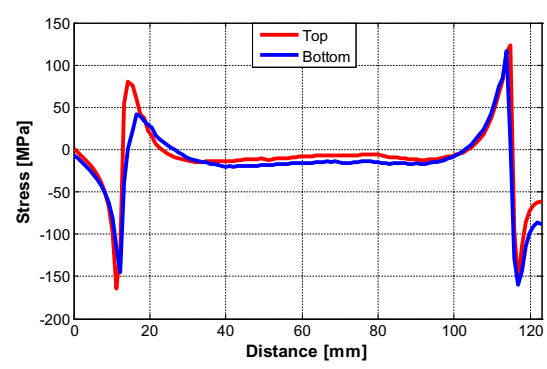

Fig. 9. Transverse residual stress. Plate set I.

4.1.2. Plate set VII

A dissimilar distribution appears due to the different thicknesses (Fig. 10). The peak value is approximately the same as verified in plate set I. Further details of this work may be found in [7].

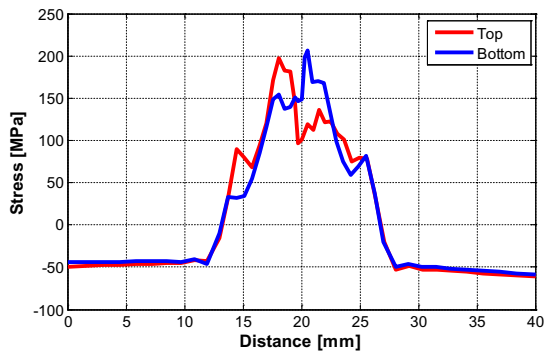

Fig. 10. Longitudinal residual stress. Plate set VII.

Top surface stress values are positive along the weld line. A non-uniformity, caused by thickness change, increases the disparities between the residual stresses measured (Fig. 11).
Residual stress distribution is not symmetric. The highest values at base occur in AA6082 plate and at top occur in AA5083 plate. Using these different aluminium alloy plates increase peak values and decreases compressive values. The tensile stress area is smaller and the stress relief is more evident at the surface.

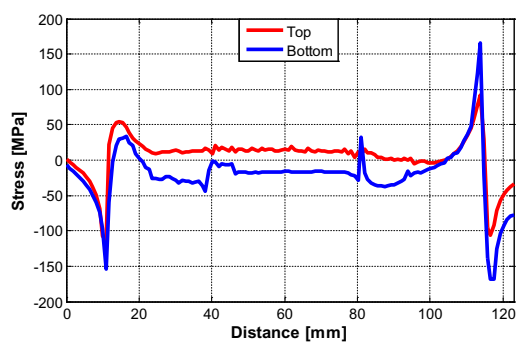

Fig. 11. Transverse residual stress. Plate set VII.

4.1.3. Plate set VIII

As shown along this section, the transverse residual stress is essentially compressive. It results in similar deformed shapes in all sets.
Figs. 8 and 12 show a twin peak residual stress distribution also found in experimental work as Braga *et al.* [10], where metallurgic transformations lead to stress relief in the centre of the welding [11].
Buckling tendencies of thin plates in the presence of residual stresses resulted in difficulties to predict the deformed shape.

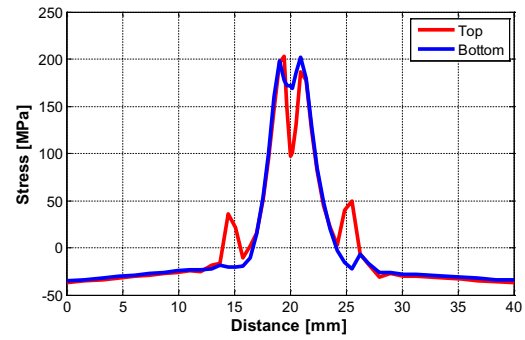

Fig. 12. Longitudinal residual stress. Plate set VIII.

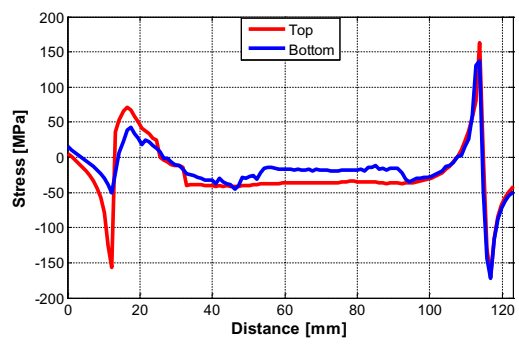

Fig. 13. Transverse residual stress. Plate set VIII.

5. Conclusions

The results shown in the previous section include approximations such as simplified boundary conditions, welding parameters, unknown weld bead geometry and FE meshes that may be improved. It was not possible to verify the residual stresses by experimental tests. Despite these limitations, it was possible to observe that the usual schematic longitudinal residual stress distribution in butt joints, as presented *e.g.* by Masubuchi [4], has a shape that is not realistic enough since it does not include the twin peak distribution found in experiments and in the present FE modelling.

Acknowledgements

The authors would like to acknowledge EDAETECH and André X. F. da Silva for delivering the samples and ESI Madrid for the technical support.

References

[1] Y. Xiaohong, S. Yonglunb, R. Guowei, X. Tianjiao, Adv. Mater. Res. 383-390 (2012) 1801.
[2] ESI Group, Weld distortion and weld quality simulation. Benefits, capabilities and products, Sysweld Toolbox (2010).
[3] D. Tikhomirov, B. Rietman, K. Kose, M. Makkink, Adv. Mater. Res. 6-8 (2005) 195.
[4] K. Masubuchi (Ed.), Analysis of Welded Structures: Residual Stresses, Distortion, and their Consequences, Pergamon Press, USA, 1980, p.192.
[5] Canadian Welding Bureau (Ed.), Welding for Design Engineers, Residual Stress and Distortion, Gooderham Centre for Industrial Learning, Mississauga, Ontario, Canada, 2006, p. 257.
[6] M.F. Zaeh, S. Roeren, Adv. Mater. Res. 10 (2006) 133.
[7] T.R. Lima, MSc thesis, Faculdade de Engenharia da Universidade do Porto, Porto, Portugal, 2014.
[8] M. Zain-ul-Abdein, D. Nélias, J.-F. Jullien, D. Deloison, Int. J. Mater. Form. 1(S1) (2008) 1063.
[9] M. Zain-ul-Abdein, D. Nélias, J.-F. Jullien, D. Deloison, J. Mater. Process. Technol. 209 (2009) 2907.
[10] D.F.O. Braga, H.E. Coules, T. Pirling, V. Richter-Trummer, P. Colegrove, P.M.S.T. de Castro, J. Mater. Process. Technol. 213 (2013) 2323.
[11] T. Kannengiesser, A. Kromm, Rev. Soldagem Inspecao 14(1) (2009).